Counterintuitive dispersion effect near surface plasmon resonances in Otto structures

Lin Wang,[1] Li-Gang Wang,[1,2,*] Lin-Hua Ye,[1] M. Al-Amri,[3,4] Shi-Yao Zhu,[2] and M. Suhail Zubairy[2,4]
[1]*Department of Physics, Zhejiang University, Hangzhou 310027, China*
[2]*Beijing Computational Science Research Center, Beijing, 100084, China*
[3]*The National Center for Applied Physics, KACST, P. O. Box 6086, Riyadh 11442, Saudi Arabia*
[4]*Institute for Quantum Science and Engineering (IQSE) and Department of Physics and Astronomy, Texas A&M University, College Station, Texas 77843-4242, USA*
(Received 19 January 2016; published 5 July 2016)

In this paper, we investigate the counterintuitive dispersion effect associated with the poles and zeros of reflection and transmission functions in an Otto configuration when a surface plasmon resonance is excited. We show that the zeros and/or poles in the reflection and transmission functions may move into the upper-half complex-frequency plane (CFP), and these locations of the zeros and poles determine the dispersion properties of the whole structures (i.e., the frequency-dependent change of both reflected and transmitted phases). Meanwhile, we demonstrate various dispersion effects (both normal and abnormal) related to the changes of the poles and zeros in both reflection and transmission functions when considering the properties of metal substrates. For a realistic metal substrate in an Otto structure, there are the optimal thickness and incident angle, which correspond to the transitions of the zeros in the reflection function from the upper-half to lower-half CFP. These properties may be helpful to manipulate light propagation in optical devices.

DOI: 10.1103/PhysRevA.94.013806

I. INTRODUCTION

The propagation of light pulses in dispersive media and optical devices is an interesting topic in physics and has been explored extensively for several decades [1,2]. It is well known that the dispersion of light usually exists in various materials and structures and is often associated with absorption or dissipation. The relations between the dispersion and absorption (or dissipation) of materials or between the amplitude and phase in transfer functions of optical devices are usually described by the conventional Kramers–Kronig (CKK) relations [3,4], which are very important to determine dispersion in experiments by directly measuring its corresponding absorption or transmitted spectra. Traditionally, the dispersion inside a spectral dip is anomalous, which leads to the superluminal propagation, while it is normal inside a spectral peak, which corresponds to the subluminal propagation.

However, there are some unexceptional situations that are invalid for CKK relations. For examples, there exists the complicated change of phase accompanied by uniform-intensity transmission for all frequencies in the Gires–Tournois interferometer [5,6]. Meanwhile, the dispersion can exhibit different behavior (from normal to abnormal) under different parameters and, even there, CKK relations do not exist for a birefringent filter [6,7]. In 2002, Wang [8] found the dispersive behavior opposite to that of a Lorentz oscillator in a linear and causal system when gain or loss media are introduced. Heebner and Boyd [9] found exotic optical properties including subluminal and superluminal group velocities in a device constructed of a sequence of microresonators coupled to an optical waveguide, in which both normal and abnormal dispersion may appear near the spectral dip [9,10]. Later, Chang and Smith [11] further considered gain-assisted superluminal propagation in coupled optical resonators. Most recently, we demonstrated the counterintuitive dispersion effect in gain slabs that the peaks (dips) in the gain spectrum correspond to abnormal (normal) dispersion [12]. In all these investigations, there is a common feature: the poles and/or zeros of transfer functions (reflection and transmission coefficients of light) may move into the upper-half complex-frequency plane (CFP), which essentially leads to exotic dispersion not obeying the CKK relations.

Optical surface plasmon resonances (SPRs) are the result of the interaction of light with free electrons at a metal-dielectric interface [13]. The energy of light may transfer to the collective excitations of free electrons under certain conditions. There are unique features of SPRs, such as the enhancement of localized electromagnetic fields and highly sensitive plasmons. Thus, SPRs are expected to be applied in the sensing and detection of chemicals, biological agents, and phase transitions [14–16] (for a review in biosensing, see Ref. [17]). Meanwhile, various strategies are proposed to excite SPRs, such as grating couplers [18], waveguides couplers [19], fiber-optic couplers [20], and prism couplers [21,22]. The Kretschmann configuration [21] and the Otto configuration [22], which belong to the frustrated total internal structure, are two typical prism couplers and the corresponding dispersion relations are studied extensively [23–26]. These investigations have concentrated on the dispersion relations and the properties of the different modes. Through the dispersion relations, the optical characteristics of the two prism couplers have also been analyzed, including the propagation length, the penetration depth, field enhancement, Goos–Hänchen shift and the amplitude and phase variation [27–30]. In 2000, researchers noticed poles in the upper-half CFP in the photon's tunneling through frustrated total internal reflection [31]. In earlier literature [32], Depine *et al.* used the concept of complex thickness to solve the singularity of reflection in film systems. Recently, Zeller *et al.* [33,34] used the similar method to obtain the critical coupling for positive or negative

*sxwlg@yahoo.com

Goos–Hänchen shifts in Kretschmann (or Otto) systems containing metamaterials. In this paper, we focus on the zeros and poles of the complex frequency in the transfer functions (reflection and transmission) to reveal that the counterintuitive dispersion effect exists due to the presence of the zeros and poles in the upper-half CFP for an Otto configuration. By analyzing the movements of "zero" or "poles" in the transfer functions, the behavior of the corresponding optical properties, including the amplitude, the phase, and group delay of reflected and transmitted pulse, are characterized. Moreover, we present the approach to control the transition between the conventional and counterintuitive dispersion effects near the SPRs. It may be useful to design the optical devices and control the pulse propagation.

The whole paper is organized as follows: In Sec. II, we present the theoretical model and formula of the wave propagation in the Otto configuration. In Sec. III, we discuss the change of the zero and pole points in the reflection and transmission coefficients and the corresponding dispersion relations, which lead to the controlling of the group delays of light pulses passing through the system. Finally, we present a brief summary in the Sec. IV.

II. THEORETICAL MODEL AND FORMULA

The Otto configuration, as shown in Fig. 1, consists of a prism with large relative dielectric constant ε_1 and a metal substrate with relative permittivity ε_3, and the prism and metal are separated by an air (or vacuum) gap with permittivity $\varepsilon_2 = 1$ and thickness d. Let a transverse-magnetic (TM) plane-wave light pulse be injected into the structure from the prism side at an angle of incidence θ. Here, the transmitted light is the evanescent wave, and it may be enhanced by the excitation of a surface plasmon along the air-metal interface. For simplicity but without loss of generality, we neglect the dissipation (or absorption) of the prism and assume that the angle of incidence θ is larger than the critical angle θ_c for total internal reflection.

From Maxwell's equations and boundary conditions, the reflection and transmission coefficients can be expressed as [35–37]

$$r = \frac{(p_1+p_2)(p_2-p_3)e^{-k\eta_a d} + (p_1-p_2)(p_2+p_3)e^{k\eta_a d}}{(p_1-p_2)(p_2-p_3)e^{-k\eta_a d} + (p_1+p_2)(p_2+p_3)e^{k\eta_a d}}, \tag{1}$$

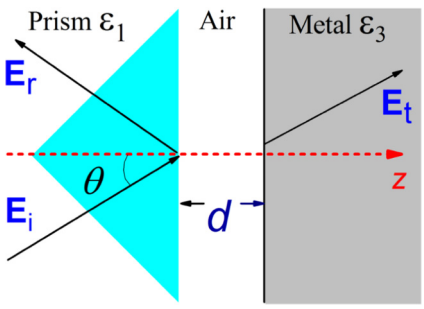

FIG. 1. Schematic of an Otto configuration consisting of the prism, air (or vacuum) gap, and metal substrate. The permittivities of prism, air, and metal are ε_1, $\varepsilon_2 = 1$, and ε_3, respectively, and d is the thickness of the air (or vacuum) gap.

$$t = \frac{4p_1p_2}{(p_1-p_2)(p_2-p_3)e^{-k\eta_a d} + (p_1+p_2)(p_2+p_3)e^{k\eta_a d}}, \tag{2}$$

where $k = \omega/c$ is the wave number of light in vacuum, $p_1 = (\varepsilon_1 - k_y^2/k^2)^{1/2}/\varepsilon_1$, $p_2 = i\eta_a/\varepsilon_2$, $p_3 = i\eta_b/\varepsilon_3$, $\eta_a = (k_y^2/k^2 - \varepsilon_2)^{1/2}$, $\eta_b = (k_y^2/k^2 - \varepsilon_3)^{1/2}$, $k_y = k\varepsilon_1^{1/2}\sin\theta$ is the wave number in the y direction, and c is the light speed in vacuum. The transmission coefficient t stands for the ratio of the magnetic field on the air-metal interface to the incoming magnetic field in the prism. These coefficients (both r and t) can be rewritten in exponential form [38,39] as $F(\omega) = e^{\ln|F(\omega)| + i\phi_F(\omega)}$, where F denotes r or t, and $|F(\omega)|$ and $\phi_F(\omega)$ are the amplitude and phase of these functions, respectively. In complex-frequency space, when all "poles" and "zeros" of these functions (r and t) are usually located at the lower-half CFP, then the amplitude and phase can be transformed into each other via the following relations [3,40,41]:

$$\ln|F(\omega)| = -\frac{\omega^2}{\pi}P\int_{-\infty}^{\infty}\frac{\phi_F(\nu)}{\nu(\nu^2-\omega^2)}d\nu, \tag{3}$$

$$\phi_F(\omega) = \frac{\omega}{\pi}P\int_{-\infty}^{\infty}\frac{\ln|F(\nu)|}{\nu^2-\omega^2}d\nu, \tag{4}$$

where P denotes the Cauchy integral principal value. In all our discussion, we call these two equations the CKK relations. Here we emphasize that, as pointed out in literatures [3,5,6,8], the violation of Eqs. (3) and (4) does not imply the violation of causality. From Eqs. (1) and (2), if the zeros and poles in these functions exist, they should, respectively, satisfy the solutions of the following equations:

$$(p_1+p_2)(p_2-p_3)e^{-k\eta_a d} + (p_1-p_2)(p_2+p_3)e^{k\eta_a d} = 0, \tag{5}$$

$$(p_1-p_2)(p_2-p_3)e^{-k\eta_a d} + (p_1+p_2)(p_2+p_3)e^{k\eta_a d} = 0, \tag{6}$$

in the complex-frequency domain. In the discussion below, we assume ε_1 is a real positive constant. In fact, when Eq. (6) is held within the real frequency domain, its solution corresponds to the dispersion equation of surface plasmons [42,43]. When $d = 0$, the dispersion relation for a single dielectric-metal interface can be readily obtained: $\varepsilon_1/k_{1z} + \varepsilon_3/k_{3z} = 0$, where $k_{1z} = (k^2\varepsilon_1 - k_y^2)^{1/2}$, and $k_{3z} = (k^2\varepsilon_3 - k_y^2)^{1/2}$ through solving Eq. (6). Within this paper, we use the prism coupling to excite the surface plasmon. Since light cannot pass through the metal substrate, the result discussed below should be experimentally verified by the reflection of light. Next we discuss the different situations for different ε_3.

Case 1. When ε_3 is a real constant (i.e., no loss for the metal), then the solutions of the complex frequencies ($\tilde{\omega}_{z,p} = \omega_{z,p}^r + i\omega_{z,p}^i$), corresponding to the zeros and poles in Eqs. (5) and (6), can be obtained analytically. For the cases of the angle of incidence obeying $\sin^2\theta < \frac{|\varepsilon_3|}{\varepsilon_1|1+\varepsilon_3|}$, these solutions are, respectively, given by

$$\omega_z^r = \frac{c}{\eta_a d}\tanh^{-1}\left(-\frac{\varepsilon_3\eta_a}{\eta_b}\right), \quad \omega_z^i = \frac{c}{\eta_a d}\tan^{-1}\left[\frac{\eta_a}{p_1}\right], \tag{7}$$

$$\omega_p^r = \frac{c}{\eta_a d}\tanh^{-1}\left(-\frac{\varepsilon_3\eta_a}{\eta_b}\right), \quad \omega_p^i = -\frac{c}{\eta_a d}\tan^{-1}\left[\frac{\eta_a}{p_1}\right]. \tag{8}$$

For the cases of the angle of incidence satisfying $\sin^2\theta > \frac{|\varepsilon_3|}{\varepsilon_1|1+\varepsilon_3|}$, the solutions become

$$\omega_z^r = \frac{c}{\eta_a d}\tanh^{-1}\left(-\frac{\eta_b}{\varepsilon_3\eta_a}\right), \quad \omega_z^i = -\frac{c}{\eta_a d}\tan^{-1}\left[\frac{p_1}{\eta_a}\right], \tag{9}$$

$$\omega_p^r = \frac{c}{\eta_a d}\tanh^{-1}\left(-\frac{\eta_b}{\varepsilon_3\eta_a}\right), \quad \omega_p^i = \frac{c}{\eta_a d}\tan^{-1}\left[\frac{p_1}{\eta_a}\right], \tag{10}$$

whereas for the case $\sin^2\theta = \frac{|\varepsilon_3|}{\varepsilon_1|1+\varepsilon_3|}$, both ω_z^r and ω_p^r tend to be infinite values with $\omega_z^i = \omega_p^i = 0$ in Eqs. (5) and (6). Clearly, both the zeros and poles for the reflection and transmission coefficients can be located in the lower-half or upper-half CFP. Once these zeros and poles move into the upper-half complex-frequency plane, Eqs. (3) and (4) are invalid. Therefore, as in Ref. [12], counterintuitive dispersion effects are expected.

Case 2. When ε_3 is a complex constant (i.e., with the loss or gain for the metal), the analytical solutions of Eqs. (5) and (6) can be formally expressed as

$$\tilde{\omega}_z = \frac{c}{2\eta_a d}\ln\left[\frac{(p_1+p_2)(p_3-p_2)}{(p_1-p_2)(p_3+p_2)}\right], \tag{11}$$

$$\tilde{\omega}_p = \frac{c}{2\eta_a d}\ln\left[\frac{(p_1-p_2)(p_3-p_2)}{(p_1+p_2)(p_3+p_2)}\right]. \tag{12}$$

Here the function "ln" is calculated in the complex domain. Now the solutions seem to be more complicated than those in Case 1. In fact, the solutions of Case 1 are the special case. Therefore, there are also the possibilities that the zeros and poles are located in the upper-half CFP. We discuss them in detail in the next section.

Case 3. When the metal substrate is in general a dispersive medium, i.e., ε_3 is a function of frequency, then Eqs. (5) and (6) have to be solved numerically. Similar to the two cases discussed above, we show below the locations of the zeros and poles in the CFP.

Meanwhile, in order to observe experimentally the dispersion effect due to the violation of Eqs. (3) and (4), we can measure the group delay of a light pulse reflected from the system that we have considered. We assume that the incident pulse is a Gaussian pulse with a very narrow spectrum, i.e., $\Delta\omega \ll \omega$, where $\Delta\omega$ is the spectral width of the pulse, so that the reflected pulse suffers minimal distortion. In this situation, the group delay of the reflected light is defined by [44–47]

$$\tau_r = \frac{d\phi_r}{d\omega}, \tag{13}$$

where ϕ_r is the phase of the reflection coefficient in Eq. (1). Using the reflection coefficient, we can also express the group delay as follows [48]:

$$\tau_r = \frac{1}{|r|^2}\left[\mathrm{Re}[r]\frac{d\mathrm{Im}[r]}{d\omega} - \mathrm{Im}[r]\frac{d\mathrm{Re}[r]}{d\omega}\right]. \tag{14}$$

Therefore the group delay of pulse propagations can be obtained in our systems which may be helpful for the experimental verification. Similarly, the behavior of the transmitted light in the metal substrate could be described by its transmitted group delay from transmission coefficient t as [48]

$$\tau_t = \frac{1}{|t|^2}\left[\mathrm{Re}[t]\frac{d\mathrm{Im}[t]}{d\omega} - \mathrm{Im}[t]\frac{d\mathrm{Re}[t]}{d\omega}\right]. \tag{15}$$

Although this physical quantity cannot be measured directly, it is meaningful to analyze the properties of the poles changing from the lower-half to the upper-half in the complex-frequency plane.

III. RESULTS AND DISCUSSIONS

From the above calculation and discussion, we note that there are both poles and zeros in reflection coefficients, while there are only poles in the transmission coefficients. All these poles and zeros can move from the lower-half to upper-half CFP (or vice versa) under certain conditions. In this section, we show systematically the influence of the metal's permittivity on the locations of the imaginary parts of the poles and zeros for the Otto configuration and demonstrate the dramatic change of dispersion due to the location change of these poles and zeros. We also discuss in detail the corresponding properties of group delays for light reflection and transmission. In the following calculation, without loss of generality, the parameters of the systems are taken as follows: $\varepsilon_1 = 9$ (for a prism, which means that the critical angle of total reflection is $\theta_c = 19.47^\circ$), and $d = 0.5\ \mu$m for the air gap.

A. Constant ε_3

In this section, we first consider the simple case in which ε_3 is a complex constant. Thus we can use the results in cases 1 and 2 discussed in Sec. II. The behavior of light passing through such Otto structures can be determined by the locations of these zeros and poles in reflection and transmission functions. To have a complete understanding of the problem, we assume that the metal parameter ε_3 is an arbitrary complex constant, including both the absorbing or gain cases.

In Fig. 2 we show different regions of zeros and poles of reflection and transmission functions in the complex frequency domain. It is clearly seen that, under different angles of incidence, the locations of these zeros and poles in the complex frequency domain are different. When θ is slightly larger than the total internal reflection angle (θ_c) [see Fig. 2(a)], there are four combinations denoted by four regions: Region I is for $\omega_z^i < 0$ and $\omega_p^i > 0$, Region II is for $\omega_z^i < 0$ and $\omega_p^i < 0$, Region III is for $\omega_z^i > 0$ and $\omega_p^i < 0$, and Region IV is for $\omega_z^i > 0$ and $\omega_p^i > 0$. At a certain angle of incidence, there are only two combinations, denoted Regions I and III [see Fig. 2(b)], since the transitions for the solutions of Eqs. (11) and (12) are overlapped in the complex-ε_3 space. For an angle

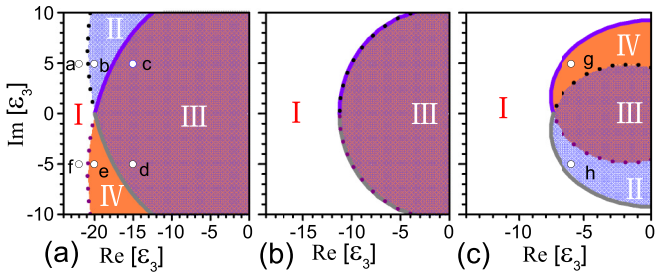

FIG. 2. Locations of zeros and poles in the complex-frequency domain as a function of complex ε_3 under different angles of incidence. (a) $\theta = 20^\circ$, (b) $\theta \sim 20.439^\circ$, and (c) $\theta = 21^\circ$. Here, Region I is for $\omega_z^i < 0$ and $\omega_p^i > 0$, Region II is for $\omega_z^i < 0$ and $\omega_p^i < 0$, Region III is for $\omega_z^i > 0$ and $\omega_p^i < 0$, and Region IV is for $\omega_z^i > 0$ and $\omega_p^i > 0$. The solid (or short-dashed) curves between regions denote the smooth (or sudden) changes of ω_z^i and ω_p^i. The parameters are $\varepsilon_1 = 9$, and $d = 0.5$ μm. Points a–h in panels (a) and (c) are located in different regions and are used in Fig. 3.

of incidence larger than that special angle, there are four combinations again [see Fig. 2(c)] and, in this situation, the locations of Regions II and IV are opposite to the case in Fig. 2(a).

Let us discuss Fig. 2(a) in detail. From regions I to II, the locations of the poles change suddenly from the upper-half to lower-half CFP, and the boundary between regions I and II for the poles, denoted by the black short-dashed curve, is undefined in the absorbing parameter space ($\mathrm{Im}[\varepsilon_3] > 0$); while all zeros in both regions I and II are located in the lower-half CFP. In regions II and III, all poles are located in the lower-half CFP; while the zeros change continuously from the lower-half to upper-half CFP and the violet solid curve between regions II and III denotes these zeros located on the real axis of the CFP. From regions III to IV, the poles are seen to increase continuously from the lower-half to upper-half CFP and the gray solid curve between regions III and IV denotes the poles located on the real axis of the CFP; while the zeros in these regions (III and IV) are within the upper-half CFP. Lastly, the zeros also change suddenly from the upper-half to lower-half CFP from the regions IV to I, and similarly the boundary between the regions IV and I for the zeros, denoted by the purple short-dashed curve, is undefined in the gain parameter space ($\mathrm{Im}[\varepsilon_3] < 0$), but the poles in both regions I and IV are located at the upper-half CFP. It should be pointed out that, when the zeros are located on the real axis of the complex frequency, there is no reflected light at all and it is meaningless to calculate the dispersion or the group delay. For the poles, there are no possibilities to be located on the real axis of the CFP in the absorbing parameter space ($\mathrm{Im}[\varepsilon_3] > 0$). Our motivation here is to emphasize that the changes of the zeros or poles leads to the change of dispersion as discussed below.

Similarly, in Fig. 2(b), under a suitable angle of incidence, regions II and IV disappear due to the accidental overlap of the solid and short-dashed curves. Thus there are only two regions (I and III). In the absorbing parameter space, the transition from regions I to III for the poles is discontinuous from the upper-half to lower-half CFP while for the zeros it changes smoothly from the lower-half to upper-half CFP. In contrast, in the gain parameter space, the transition from regions I to III for the poles changes smoothly from the upper-half to lower-half CFP but for the zeros it changes abruptly from the lower-half to upper-half CFP.

From the discussion above, one can now understand clearly the behavior of the poles and zeros in Fig. 2(c). The most important feature is that the poles and zeros of both reflection and transmission coefficients, depending on the value of ε_3, can be located at the upper- or lower-half CFP. Therefore, it is expected that the corresponding light propagation through such structures differs significantly. Next we demonstrate that the property of dispersion is determined completely by the locations of the poles or zeros, which in turn affect the group delay of a reflected (or transmitted) pulse of light. As we have known from the CKK relations that all the poles and zeros in transfer functions (reflection and transmission coefficients) are usually located at the lower-half CFP. This leads to the criterion of dispersion that a peak (or dip) in both reflected and transmitted spectral lines simply corresponds to a normal (or abnormal) dispersion. However, once the poles or zeros of transfer functions move into the upper-half CFP, the CKK relations are invalid and the above criterion can no longer be applied. In this sense, we refer to the effect of such dispersions violating the CKK relation as the counterintuitive dispersion effect.

In Fig. 3 we show the typical properties of dispersion and the corresponding group delays when ε_3 is located at different regions. In Fig. 3(a), it is seen that a peak in the transmitted spectrum corresponds to an abnormal dispersion (the decrease of phase) with a negative group delay and the CKK relations for t are invalid, because the pole is located in the upper-half CFP [see Fig. 2(a)]; but a dip in the reflected spectrum still corresponds to the abnormal dispersion with a negative group delay, although r contains a pole in the upper-half CFP and a zero in the lower-half CFP [see Fig. 2(a)]. In Fig. 3(b), for the pole of t changes into the lower-half CFP, the peak in $|t|$ corresponds to normal dispersion (the increase of phase) with a positive group delay, which obeys the above dispersion criterion, so that the CKK relations are valid; meanwhile the zero of r is still located at the lower-half CFP, the properties of r (its dispersion and group delay) are the same as in Fig. 3(a). In Fig. 3(c), because the zero of r moves into the upper-half CFP, the dip in $|r|$ corresponds to the normal dispersion accompanied by a positive group delay and here the CKK relations for r are also invalid; however, both the dispersion and the CKK relations for t are the same as in Fig. 3(b). Thus, for the cases of $\mathrm{Im}[\varepsilon_3] > 0$ [see Figs. 3(a)–3(c) and Fig. 2(a)], it can be seen that the zero of r only determines the behavior of the reflected light and the pole of transmission coefficient only determines the behavior of the transmitted light.

However, assume that the metal's parameter ε_3 can be gain, i.e., $\mathrm{Im}[\varepsilon_3] < 0$, the properties of transfer functions become more interesting (although gain metals do not exist naturally but might be fabricated artificially in the future). In Fig. 3(d), the peaks in r and t correspond to the normal dispersion and these properties also seem to obey the above dispersion criterion, but in this case the zero of r is located at the upper-half CFP and the poles of r and t are located at the lower-half CFP [see Fig. 2(a)]. In Fig. 3(e), both the peaks in r and t correspond to the abnormal dispersion and

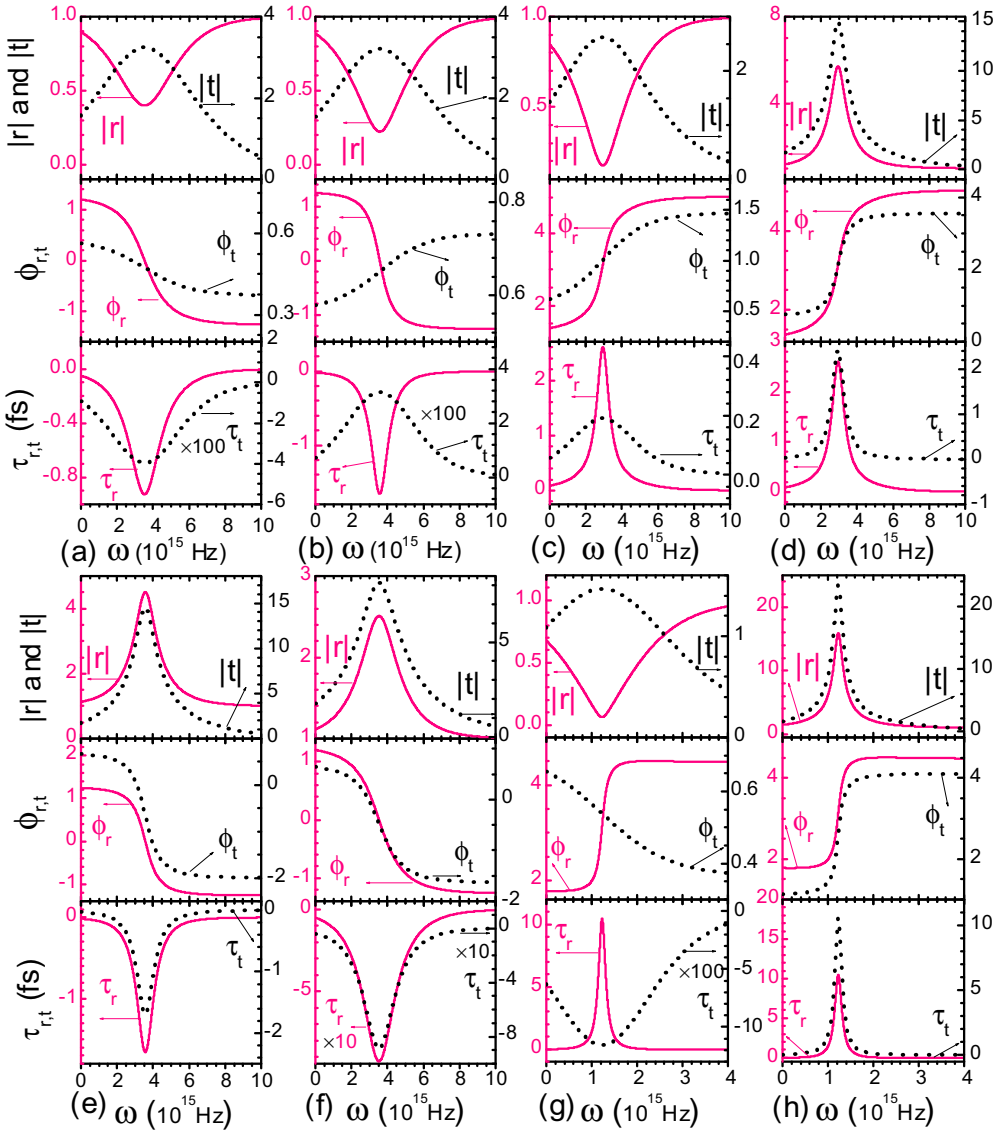

FIG. 3. Typical properties of the amplitude and phase of the reflection (solid lines) and transmission (dashed lines), and their corresponding group delays under different situations: from panels (a) to (f): $\varepsilon_3 = -22 + i5$, $-20 + i5$, $-15 + i5$, $-15 - i5$, $-20 - i5$, $-22 - i5$, respectively, with $\theta = 20^\circ$, and from panels (g) to (h): $\varepsilon_3 = -6 + i5$, $-6 - i5$, respectively, with $\theta = 21^\circ$. All these values of ε_3 are denoted by points a–h in Fig. 2; the other parameters are the same as in Fig. 2.

negative group delays, and now all these properties violate the above dispersion criterion again since the poles of r and t move into the upper-half CFP but the zero of r is still in the upper-half CFP [see Fig. 2(a)]. In Fig. 3(f), the dispersion for r and t is the same as in Fig. 3(e), but now the zero of r changes to be in the lower-half CFP. Obviously, for all these gain cases of $\mathrm{Im}[\varepsilon_3] < 0$, the properties of both r and t and their dispersion are only determined by their poles, and the zero of r does not affect the behavior of the reflected light. These properties are similar to the results in our recent work for gain slabs [12].

Similarly, we can readily understand the properties of the reflected and transmitted light in Figs. 3(g) and 3(h). The dip in r leads to a sharp normal dispersion [see Fig. 3(g)] because of $\omega_z^i > 0$ [see Fig. 2(c)], while the behavior of the transmitted light in Fig. 3(g) is similar to the case of Fig. 3(a) because of $\omega_p^i > 0$. In Fig. 3(h), due to $\omega_p^i < 0$ under the cases of $\mathrm{Im}[\varepsilon_3] < 0$, it is expected that both the peaks of r and t correspond to the normal dispersion with positive group delays. Here, we should emphasize that the magnitude maximum in transmission peak usually corresponds to the excitation of the surface plasmon under a certain angle of incidence larger than that of the internal reflection in the prism. These poles do not lead to the infinite transmission since they are in general located at lower-half or upper-half CFP. In the next section, it shows that all the poles are actually located at the lower-half CFP for the absorptive systems.

In addition, when ε_3 becomes a real number, i.e., there is no absorption (or gain), then it is seen that there are only two regions (see regions I and III in Fig. 2 along the real axis of ε_3). The properties of both the reflected and transmitted light in this situation are similar to those in Figs. 3(a) and 3(c), except for the amplitude $|r|$, which is always equal to unity under the condition of total internal reflection.

It should also be mentioned that there is a phase-matching condition to excite the surface plasmons in this Otto configuration. For real ε_3, the phase-matching condition is $\sin^2\theta = \frac{|\varepsilon_3|}{\varepsilon_1|1+\varepsilon_3|}$. For a complex ε_3, this condition is the solution of Eq. (6), and in this situation it differs from the solution of Eq. (5) for the zeros.

B. Dispersive ε_3

As pointed out in Ref. [8], in general, a Lorentz medium has poles but not zeros in the complex transmission, whereas resonators may have both poles and zeros. If there are no zeros in the transfer functions, the change of reflected and transmitted dispersion relations is the consequence of the movement of the poles like the situations in Ref. [12]. In our above calculations, it was shown that both poles and zeros of complex transfer functions may coexist in the upper-half CFP for the Otto systems with constant ε_3, and the transmission is only affected by the poles of the transmitted function.

Now let us consider the general cases that the realistic metal substrate ε_3 contains both absorption and dispersion. The relative permittivity ε_3 can be described as a Drude model,

$$\varepsilon_3 = 1 - \frac{\omega_p^2}{\omega^2 + i\gamma\omega},$$

where ω_p and γ are the plasma and damping frequencies, respectively. This model is suitable for many usual metals [49]. The results of our following example are suitable for the cases of other metals. The only difference is that the similar effects happen in different frequency regions for other metals.

Here we take the metal silver (Ag) as a typical example. According to Ref. [49], the optical parameters of Ag are $\omega_p = 1.3926 \times 10^{16}$ Hz and $\gamma = 3.18712 \times 10^{13}$ Hz. Due to the frequency dependence of ε_3, Eqs. (11) and (12) are hard to be solved directly and they should be solved numerically. To know the locations of the zeros and poles for the reflection and transmission functions, Eqs. (11) and (12) can be transformed into the forms

$$d = \frac{c}{2\eta_a\tilde{\omega}_z}\ln\left[\frac{(p_1+p_2)(p_3-p_2)}{(p_1-p_2)(p_3+p_2)}\right],$$
$$d = \frac{c}{2\eta_a\tilde{\omega}_p}\ln\left[\frac{(p_1-p_2)(p_3-p_2)}{(p_1+p_2)(p_3+p_2)}\right].$$

Requiring d to be a positive and real quantity in these two equations, one can readily obtain the locations of the zeros and poles in the CFP.

In Fig. 4, we demonstrate the locations of these zeros (solid line) and poles (dashed line) for this Otto configuration with the Ag substrate. In Fig. 4, we see that the location of the zeros can change from the lower-half to upper-half CFP, while for the poles, it can change only within the lower-half CFP. The direction of arrows indicates the increasing change of thickness d. In principle, there is no limit on the thickness d. Every value

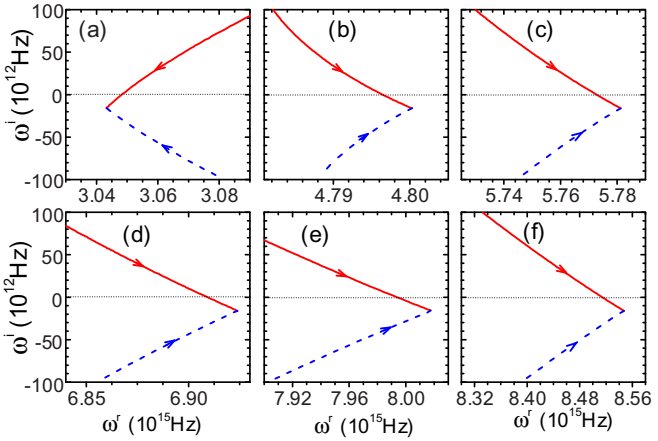

FIG. 4. Changes of the zeros (solid lines) and poles (dashed lines) in the complex-frequency domain for the existence of the real solution of thickness d in Eqs. (11) and (12) for (a) $\theta = 20^\circ$, (b) $\theta = 21^\circ$, (c) $\theta = 22^\circ$, (d) $\theta = 24^\circ$, (e) $\theta = 28^\circ$, and (f) $\theta = 32^\circ$. Here $\varepsilon_3 = 1 - \frac{\omega_p^2}{\omega^2+i\gamma\omega}$ is a dispersive silver metal with $\omega_p = 1.3926 \times 10^{16}$ Hz and $\gamma = 3.18712 \times 10^{13}$ Hz, and the direction of arrows indicates the increasing change of thickness d.

of d corresponds to a zero and a pole. For the zeros, there is a critical thickness that corresponds to the transition point from the lower-half to upper-half CFP. However, for the poles, there is no such a transition.

In Fig. 5, we further show the properties of the reflection and the corresponding movements of the imaginary parts of zeros in the reflection. We observe that there are the optimal angle (θ_{opt}) and thickness (d_{opt}) for maximally exciting the

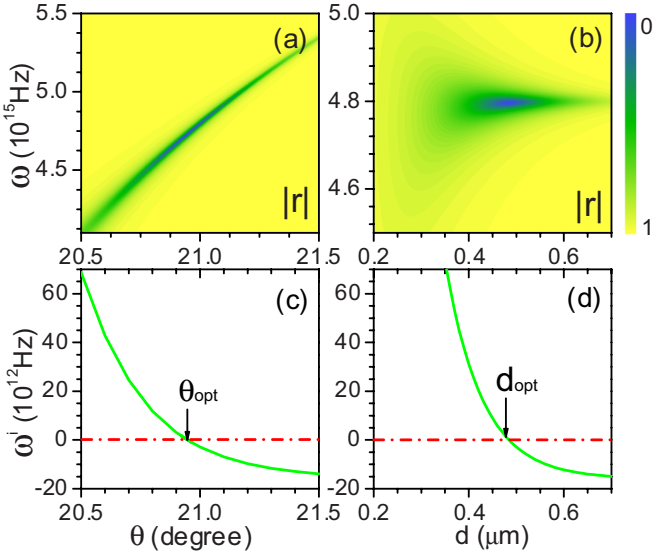

FIG. 5. The existence of the optimal angle (a) and thickness (b) from the reflection coefficient to judge the excitation of the surface-plasmon mode, which corresponds to the critical angle (c) and thickness (d) of the transition point for the zeros moving from the lower-half to upper-half CFP, respectively. The thickness is $d = 0.5\mu$m in panels (a) and (c) and the angle is $\theta = 21^\circ$ in panels (b) and (d). Other parameters are the same as in Fig. 4.

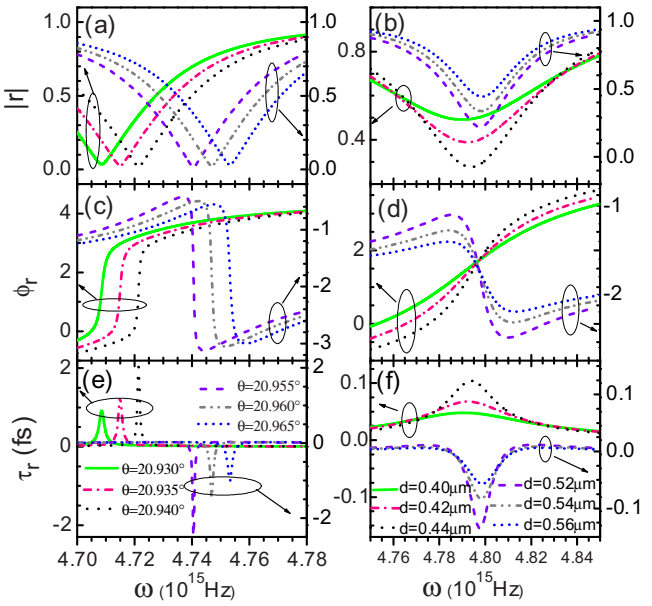

FIG. 6. The typical properties of the reflectivity $|r|$, its phase ϕ_r, and the reflected group delay τ_r under different situations. Note that solid, dash-dotted, dotted, dashed, dash dot dotted, and short dashed lines denote the case $\theta = 20.930^\circ, 20.935^\circ, 20.940^\circ, 20.955^\circ, 20.960^\circ$, and 20.965° in panels (a), (c), (e) and $d = 0.40\,\mu$m, $0.42\,\mu$m, $0.44\,\mu$m, $0.52\,\mu$m, $0.54\,\mu$m, and $0.56\,\mu$m in panels (b), (d), (f), respectively. The thickness is $d = 0.5\,\mu$m in panels (a), (c), (e), and the angle is $\theta = 21^\circ$ in panels (b), (d), (f). Other parameters are the same as in Fig. 4.

surface plasmons [see Figs. 5(a) and 5(b)] after including the dispersive property of the metal substrate. The optimal angle $\theta_{\rm opt}$ and thickness $d_{\rm opt}$ actually correspond to the critical angle and thickness for the zeros (in the reflection coefficient) transiting between the lower-half and upper-half CFP [see Figs. 5(c) and 5(d)]. For systems with different metals, the optimal angle and thickness are different due to the change of ω_p and γ.

Figure 6 shows the properties of the reflection, its phase, and group-delay dependence on the incident frequency under different incident angle θ in Figs. 6(a), 6(c), and 6(e) and thickness d in Figs. 6(b), 6(d), and 6(f). Although there is always a dip in $|r|$, the group delay changes dramatically from positive to negative, i.e., the dispersion is totally different before and after the corresponding critical angle or thickness, see Figs. 6(a), 6(c), 6(e) and 6(b), 6(d), 6(f). For example, as θ increases and gradually approaches $\theta_{\rm opt}$, the normal dispersion becomes steeper and steeper, thus the group delay is larger and larger. When $\theta = \theta_{\rm opt}$, the phase of reflection is undefined at the frequency of $|r| = 0$, so that it is meaningless to calculate the group delay. Once θ is larger than $\theta_{\rm opt}$, there occurs the abnormal dispersion accompanying a dramatic phase change (corresponding to a large negative group delay). There are similar phenomena as d changes; see Figs. 6(b), 6(d), and 6(f). It should be mentioned that such changes of the dispersion and the group delay could be realizable in experiments since one has demonstrated the high-precision control on the thickness or angle of incidence in the Otto configurations [22]. Therefore, for a practical Otto configuration, one can tune the properties of pulse reflection by adjusting the angle of incidence or the thickness.

Lastly, it should be pointed out that such counterintuitive dispersion effects determined by the movement of the poles or zeros of the transfer functions in CFPs may also be explained by the coupling mechanism. According to Ref. [22], the internal and radiation dampings around the SPR coexist in the system. The former, caused by the energy absorption in the metal, is proportional to the imaginary part of ε_3, and the latter, induced by the emission of waves into the prism by the SPR, is strongly dependent on the thickness d of the air gap. That is, one can manipulate the radiation damping by changing the value of d in experiments. Like in the Kretchmann configuration [50,51], when the internal damping is greater than radiation damping, such coupling is regard as the undercoupled system, and the abnormal dispersion happens as mentioned in Refs. [9,11]. When the internal damping is chosen to be weaker than radiation damping, it becomes overcoupled and the normal dispersion occurs in the overcoupled regime. When the internal damping and radiation damping are exactly equal, which is critically coupled, then the reflection of the pulse vanishes. This d is known as the optimal thickness, as mentioned above, and the dispersion relations display the reversal behavior before and after this critical thickness.

IV. SUMMARY

We have investigated the counterintuitive dispersion effect of reflection and transmission functions in an Otto configuration as the SPR of the metal is excited. The dispersion relations may violate the CKK relations (3) and (4) since, under certain conditions, there are zeros and poles in the upper-half CFP. These relations are sensitive to the complex permittivity of the metal and the incident angle. We explain the transition of the dispersion in both lossless and lossy systems by controlling the movements of the poles and zeros in the transfer function. Furthermore, we show that there is an optimal thickness and incident angle for general systems containing dispersion and absorption. We observe that the dispersion effects have a drastically different behavior when the thickness of the gap and the angle of incidence are above and below certain critical values, respectively. Due to the existence of the optimal thickness and optimal incident angle, there is the critical coupling to control light propagation from subluminal to superluminal. Thus our results are valuable in manipulating light propagation in optical devices.

ACKNOWLEDGMENTS

This work was supported by the National Natural Science Foundation of China (NSFC) (Grants No. 11274275, No. 61078021, and No. U1330203), and grants from the National Basic Research Program of China (No. 2012CB921602 and No. 2012CB921603). It was also supported by the Fundamental Research Funds for the Center Universities (No. 2016FZA3004). This research is also supported by NPRP grant 7-210-1-032 by the Qatar National Research Fund and a grant from King Abdulaziz City for Science and Technology.

[1] L. Brillouin, *Wave Propagation and Group Velocity* (Academic, New York, 1960).

[2] K. E. Oughstun and G. C. Sherman, *Electromagnetic Pulse Propagation in Causal Dielectrics* (Springer-Verlag, Berlin, 1994).

[3] H. M. Nussenzveig, *Causality and Dispersion Relations* (Academic Press, New York, 1972).

[4] J. D. Jackson, *Classical Electrodynamics* (Wiley, New York, 1975).

[5] F. Gires and P. Tournois, C. R. Acad. Sci. Paris **258**, 6112 (1964).

[6] M. Beck, I. A. Walmsley, and J. D. Kafka, IEEE J. Quantum Electron. **27**, 2074 (1991).

[7] S. Zhu, Appl. Opt. **29**, 410 (1990).

[8] L. J. Wang, Opt. Commun. **213**, 27 (2002).

[9] J. E. Heebner and R. W. Boyd, J. Mod. Opt. **49**, 2629 (2002).

[10] H. P. Uranus, L. Zhuang, C. G. H. Roeloffzen, and H. J. W. M. Hoekstra, Opt. Lett. **32**, 2620 (2007).

[11] H. Chang and D. D. Smith, J. Opt. Soc. Am. B **22**, 2237 (2005).

[12] L.-G. Wang, L. Wang, M. Al-Amri, S.-Y. Zhu, and M. S. Zubairy, Phys. Rev. Lett. **112**, 233601 (2014).

[13] J. M. Pitarke, V. M. Silkin, E. V. Chulkov, and P. M. Echenique, Rep. Prog. Phys. **70**, 1 (2007).

[14] X. Y. Zhang, N. C. Shah, and R. P. Van Duyue, Vib. Spectrosc. **42**, 2 (2006).

[15] H. Zhang, M. H. Harpster, W. C. Wilson, and P. A. Johnson, Langmuir **28**, 4030 (2012).

[16] M. Schwind, V. P. Zhdanov, I. Zorić, and B. Kasemo, Nano Lett. **10**, 931 (2010).

[17] I. Abdulhalim, M. Zourob, and A. Lakhtakia, Electromagn. **28**, 214 (2008).

[18] C. Thirstrup, W. Zong, M. Borre, H. Neff, H. C. Pedersen, and G. Holzhueter, Sens. Actuators B: Chem. **100**, 298 (2004).

[19] J. Homola, S. S. Yee, and G. Gauglitz, Sens. Actuators B: Chem. **54**, 3 (1999).

[20] R. C. Jorgensen and S. S. Yee, Sens. Actuators B: Chem. **12**, 213 (1993).

[21] E. Kretschmann and H. Raether, Z. Naturforsch. **23 a**, 2135 (1968).

[22] A. Otto, Z. Phys. **216**, 398 (1968).

[23] E. N. Economou, Phys. Rev. **182**, 539 (1969).

[24] B. R. Yan, J. H. Lu, L. H. Kong, and X. W. Hu, Chin. Phys. B **20**, 015101 (2011).

[25] J. J. Burke, G. I. Stegeman, and T. Tamir, Phys. Rev. B **33**, 5186 (1986).

[26] M. N. Zervas, Opt. Lett. **16**, 720 (1991).

[27] Z. M. Qi, Z. Zhang, D. F. Lu, and Q. Liu, Plasmonics **8**, 1401 (2013).

[28] S. Shen, T. Liu, and J. H. Guo, Appl. Opt. **37**, 1747 (1998).

[29] X. B. Yin, L. Hesselink, Z. W. Liu, N. Fang, and X. Zhang, Appl. Phys. Lett. **85**, 372 (2004).

[30] Y. Y. Zhang, J. C. Lai, Y. Cheng, and Z. H. Li, Appl. Opt. **48**, 1262 (2009).

[31] J. J. Carey, J. Zawadzka, D. A. Jaroszynski, and K. Wynne, Phys. Rev. Lett. **84**, 1431 (2000).

[32] R. A. Depine, V. A. Presa, and J. M. Simon, J. Mod. Opt. **36**, 1581 (1989).

[33] M. A. Zeller, M. Cuevas, and R. A. Depine, Eur. Phys. J. D **66**, 1 (2012).

[34] M. A. Zeller, M. Cuevas, and R. A. Depine, J. Opt. (Bristol, U. K.) **17**, 055102 (2015).

[35] J. A. Kong, B. L. Wu, and Y. Zhang, Appl. Phys. Lett. **80**, 2084 (2002).

[36] I. V. Shadrivov, A. A. Zharov, and Y. S. Kivshar, Appl. Phys. Lett. **83**, 2713 (2003).

[37] L.-G. Wang and S.-Y. Zhu, Appl. Phys. Lett. **87**, 221102 (2005).

[38] J. S. Toll, Phys. Rev. **104**, 1760 (1956).

[39] R. H. J. Kop, P. de Vries, R. Sprik, and A. Lagendijk, Opt. Commun. **138**, 118 (1997).

[40] A. Papoulis, *The Fourier Integral and Its Applications* (McGraw-Hill, New York, 1962).

[41] A. Mecozzi, Opt. Commun. **282**, 4183 (2009).

[42] A. A. Maradudin and D. L. Mills, Phys. Rev. B **7**, 2787 (1973).

[43] N. Mattiucci, G. D. Aguanno, M. Scalora, M. J. Bloemer, and C. Sibilia, Opt. Express **17**, 17517 (2009).

[44] X. Chen and C.-F. Li, Phys. Rev. A **68**, 052105 (2003).

[45] V. S. C. Manga Rao, S. Dutta Gupta, and G. S. Agarwal, Opt. Lett. **29**, 307 (2004).

[46] X. Chen, C.-F. Li, R.-R. Wei, and Y. Zhang, Phys. Rev. A **80**, 015803 (2009).

[47] A. Sáchez-Meroño, J. Arias, and M. M. Sánchez-López, IEEE J. Quantum Electron. **46**, 546 (2010).

[48] L. G. Wang and S. Y. Zhu, Opt. Lett. **31**, 2223 (2006).

[49] P. B. Johnson and R. W. Christy, Phys. Rev. B **6**, 4370 (1972).

[50] W. P. Chen and J. M. Chen, J. Opt. Soc. Am. **71**, 189 (1981).

[51] K. Kurihara and K. Suzuki, Anal. Chem. **74**, 696 (2002).